Studies on Ca(II) Binding to γ-Carboxyglutamic Acid

USE OF THERMAL DECARBOXYLATION TO PROBE METAL ION/γ-CARBOXYGLUTAMIC ACID INTERACTIONS*

Michael R. Lewis‡, David W. Deerfield II‡, Randal A. Hoke‡, Karl A. Koehler§, Lee G. Pedersen‡, and Richard G. Hiskey‡¶

From the ‡Department of Chemistry, The University of North Carolina at Chapel Hill, Chapel Hill, North Carolina 27514 and the §Departments of Biochemistry and Surgery, Case Western Reserve University, School of Medicine, Cleveland, Ohio 44109

The thermal decarboxylation of *N*-benzyloxycarbonyl-L-γ-carboxyglutamic acid α-methyl ester ((*Z*)-L-Gla-OMe) has been studied. In the presence of increasing amounts of calcium or magnesium ions, lyophilized powders of (*Z*)-L-Gla-OMe exhibit a corresponding increase in thermal stability. Both magnesium and calcium form relatively tight, thermally stable complexes with (*Z*)-L-Gla-OMe at high metal ion concentrations. Differences between Ca(II) and Mg(II) binding are noted at low metal ion concentrations, where (*Z*)-L-Gla-OMe is in excess. Under these conditions, complex formation with Mg(II) apparently favors a 2:1 Gla-magnesium ion complex in which both Gla residues are unstable to thermal decarboxylation. Calcium ion complexes, however, are found to favor a 3:1 Gla-calcium ion complex in which 1 of the 3 Gla residues is thermally stable.

The metal ion-binding ability of several coagulation proteins (Factors II, VII, IX, and X and proteins C, S, and Z) likely resides in the properties of a unique amino acid, γ-carboxyglutamic acid (Gla).[1] Gla is formed in a post-translational, vitamin K-mediated carboxylation of specific glutamyl residues in the intact protein (1–4). The coagulation cascade can be best summarized as a series of cleavages of a zymogen (usually Gla-containing) to an activated enzyme by an enzyme complex consisting of the appropriate enzyme (serine protease, usually Gla-containing), coenzyme (organizing protein), and an acidic phospholipid surface (5). Both the assembly and activity of the enzyme complex requires the presence of Ca(II) (6). It has been observed that other metal ions (*e.g.* Mg(II), Mn(II), Tb(III), Gd(III), and Eu(III)) cannot support the blood coagulation cascade at physiologically important rates.

The differentiation between the activity of the Ca(II) and Mg(II) ion-laden, Gla-containing protein is striking since both divalent metal ions are at similar concentrations in blood (Mg(II), 0.9 mM; Ca(II), 2.4 mM) (7). Metal ion equilibrium dialysis of bovine prothrombin fragment 1 indicates there are approximately seven Ca(II) ions bound per protein molecule and the Scatchard plot shows substantial cooperativity (8). The Scatchard plot for the Mg(II) ion equilibrium dialysis, however, indicates there are approximately five ions bound per protein molecule and these ions are bound in essentially equivalent, noninteracting sites (9). Furthermore, prothrombin fragment 1 will bind to phosphatidylserine-phosphatidylcholine vesicle surfaces in the presence of Ca(II) ions, but not in the presence of Mg(II) ions (3). Although the molecular basis of this differentiation between the interaction of these divalent metal ions and Gla-containing proteins has not been fully delineated, it is known that the protein's metal ion binding affinity is associated with the malonate subunit of the Gla residues.

Thermal decarboxylation has been used in the study of carboxylate ion-metal ion interactions in Gla-containing proteins (10, 11). A report by Poser and Price (12) documented that osteocalcin ("Bone Gla Protein") is completely decarboxylated by heating a sample obtained by lyophilization from 0.05 M HCl buffer. Rate studies at several different pH values suggest that a proton source is necessary for decarboxylation. Similarly, acid hydrolysis leads to decarboxylation but base hydrolysis does not (13–15). Poser and Price have also shown that ammonium salts will function as the proton source for Gla and that these carboxylate-ammonium salts will decarboxylate at a rate comparable to the protonated carboxylic acid. A recent study (16) reported the decarboxylation of *N*-benzyloxycarbonyl-γ-carboxyglutamic acid α-methyl ester ((*Z*)-Gla-OMe) in the presence of guanidine. This study found that the 1:1 (*Z*)-Gla-OMe-guanidine complex would decarboxylate, whereas the 1:2 complex was "protected."

Any interaction which leads to displacement of protons (or ammonium ions), such as occurs in the binding of Na(I), Ca(II), or Mg(II) ions, will "protect" the γ-carboxyl groups from decarboxylation; for example, the disodium salt of Gla is thermally stable. "Protection" in this sense refers to the attenuation of decarboxylation by electrostatic and/or steric interactions. Poser and Price (12), for instance, noted that osteocalcin remained unchanged after 4 h at 110 °C when bound to hydroxylapatite. Similarly, Bajaj *et al.* (17) studied the interaction of Ca(II) ions with human prothrombin by thermal decarboxylation. Protein samples lyophilized from buffers containing Ca(II) ions showed a corresponding increase in Gla protection, resulting in a "protection profile." Bajaj *et al.* (17) inferred that the binding of two Ca(II) ions to human prothrombin protected 6 Gla residues from decarboxylation.

An important question emerges: How does a metal ion interact with a substituted malonic acid to prevent decarboxylation? Although it is apparent from the studies of Bajaj *et*

[1] The abbreviations used are: Gla, γ-carboxyglutamic acid; (*Z*)-L-Gla-OMe, *N*, benzyloxycarbonyl-L-γ-carboxyglutamic acid α-methyl ester; prothrombin fragment 1, residues 1–156 of the amino terminus of bovine prothrombin.

al. (17) and Poser and Price (12) that the Ca(II) ion-laden protein Gla residues are protected from thermal decarboxylation, it is not obvious on a molecular level as to the mechanism of this Ca(II) ion-dependent protection. The stoichiometry of the Ca(II) ion/Gla residue complex in the intact protein is difficult to ascertain because of the possibility of interactions of Gla residues with cations other than Ca(II), such as the formation of salt bridges with arginine or lysine residues. In the present work the differences in the binding of Ca(II) and Mg(II) ions with Gla were studied by thermal decarboxylation of lyophilized powders obtained from peptide and metal ion solutions.

EXPERIMENTAL PROCEDURES

General Methods and Amino Acid Analysis—The preparation of (Z)-L-Gla-OMe has been previously described (18–20). All other chemicals are commercially available and were not purified prior to use. The concentrations of the aqueous solutions containing metal ions were determined by atomic absorption spectrophotometry on a Perkin-Elmer 560 AA spectrophotometer. Using an adaptation of the analytical method of Klapper (21), high performance liquid chromatography for amino acid analysis was performed at 63 °C on a water-jacketed Bio-Rad Aminex A-9 column (4 mm × 25 cm) (Bio-Rad) using 2-propanol (2%, v/v) in sodium citrate (0.1 M, pH 3.25) as the eluent. Detection of amino acids was accomplished by the use of a fluorometric reagent, *o*-phthaldehyde (325 mg/liter, pH 10.40) with Brij-35® (3 ml/liter, Pierce Chemical Co.) as a surfactant. Fluorescence was measured at 455 nm after excitation at 360 nm. With a flow rate of 0.5 ml/min buffer (0.4 ml/min fluorometric reagent), γ-carboxyglutamic acid elutes at 11.5 min. The extent of decarboxylation was determined by the reduction in γ-carboxyglutamic acid and the corresponding increase in glutamic acid in the alkaline hydrolysates of the heated peptide/metal ion samples.

Decarboxylation of (Z)-L-Gla-OMe in the Presence of Ca(II) and Mg(II)—An appropriate amount of a solution containing the metal ion (approximately 25 mM as determined by atomic absorption) was added to an ammonium bicarbonate buffered (0.1 M, pH 7.85) solution of (Z)-L-Gla-OMe (1.00 ml, either 0.212, 2.12, or 17.5 mM). The equilibrium mixtures were frozen and lyophilized in polypropylene-lined glass reaction tubes, and the resulting powder was heated at 110 °C for 1 h *in vacuo*. After heating, the samples were hydrolyzed by dissolving the powder in sodium hydroxide solution (2 N, 1.00 ml) and heating *in vacuo* for 24 h at 110 °C. The samples were titrated to a pH of 2.2 with HCl (1 N), and the Gla/Glu ratio was determined as above.

RESULTS

The fractional protection of (Z)-L-Gla-OMe (percent Gla remaining in the lyophilized powder after heating at 110 °C for 1 h) as a function of the metal ion/peptide ratio for Ca(II) and Mg(II) is given in Figs. 1 and 2, respectively. Three different initial concentrations of (Z)-L-Gla-OMe were investigated: 0.2, 2.1, and 17.5 mM. The metal ion concentration was adjusted to give the appropriate molar ratio of metal to peptide (molar ratios: 0, 1:8, 1:4, 1:3, 1:2, 3:4, 1, 2, 4, and 8). Each data point represents the average of three separate experiments; for each experiment, duplicate determinations of the percent Gla were performed. The standard deviation for each Ca(II) ion and Mg(II) ion data point was 1.0 and 1.3% absolute error, respectively.

The $t_{1/2}$ for the decarboxylation of a lyophilized sample of the ammonium salt of (Z)-L-Gla-OMe was found to be 0.23 h ($T = 110$ °C) (Fig. 3). Under the same conditions, the $t_{1/2}$ for the powder obtained from the lyophilization of a solution of 2.0 mM peptide and 8.0 mM calcium was significantly greater than 1 day. Since significant differences were observed between the curves obtained at different peptide concentrations (Figs. 1 and 2), it was concluded that the peptide and metal did not rearrange during lyophilization.

Experimental data was analyzed by computational simulation using four reasonable equilibrium models. During this
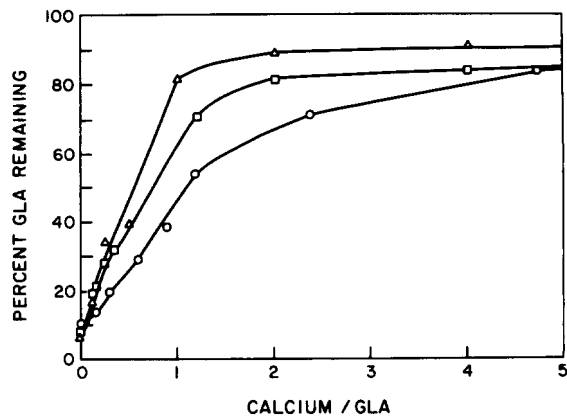

FIG. 1. **Thermal decarboxylation of (Z)-L-Gla-OMe in the presence of Ca(II).** Peptide samples at various concentrations (▲, 0.2 mM; ■, 2 mM; ●, 17 mM) were lyophilized from ammonium bicarbonate buffer (0.1 M) containing various concentrations of Ca(II) ions, sealed, and heated *in vacuo* at 110 °C for 1 h. Percent Gla remaining is presented as a function of peptide/calcium ratio present to lyophilization.
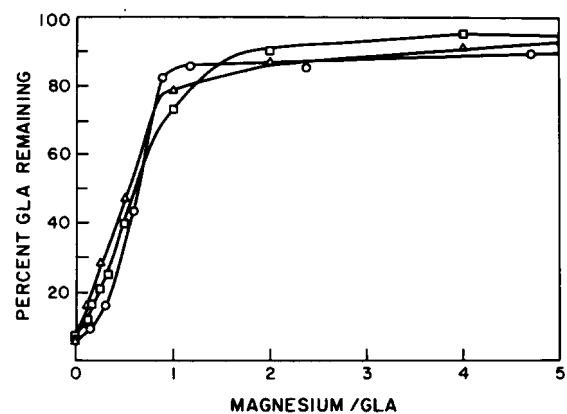

FIG. 2. **Thermal decarboxylation of (Z)-L-Gla-OMe in the presence of Mg(II).** Peptide samples at various concentrations (▲, 0.2 mM; ■, 2 mM; ●, 17 mM) were lyophilized from ammonium bicarbonate buffer (0.1 M) containing various concentrations of Mg(II) ions, sealed, and heated *in vacuo* at 110 °C for 1 h. Percent Gla remaining is presented as a function of peptide/magnesium ratio present prior to lyophilization.
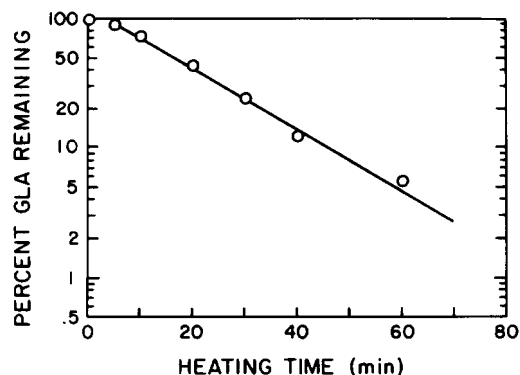

FIG. 3. **Semilogarithmic plot of percent Gla remaining versus duration of heating at 110 °C for (Z)-L-Gla-OMe.** Samples of (Z)-L-Gla-OMe (2.5 mM) were lyophilized from ammonium bicarbonate (0.1 M) and heated *in vacuo*.

process, two criteria were employed for the evaluation of a specific model: 1) how well the individual protection profiles were modeled by the calculated parameters, and 2) how consistently the equilibrium constants were reproduced for the
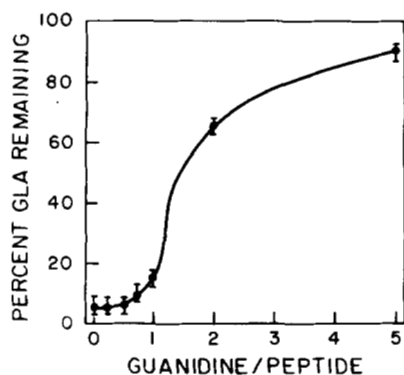
Ca(II), Mg(II) Binding to γ-Carboxyglutamic Acid

FIG. 4. **Thermal decarboxylation of (Z)-L-Gla-OMe in the presence of guanidine.** Peptide samples (2 mM) were lyophilized from ammonium bicarbonate buffer (0.1 M) containing various concentrations of guanidine, sealed, and heated *in vacuo* at 110 °C for 1 h. Percent Gla remaining is presented as a function of peptide/guanidine ratio present prior to lyophilization.

different concentrations. The latter is essential since each data set must be represented by the same set of equilibrium constants.[2]

An initial assumption in the metal ion binding simulation was that all species bound to metal ions were protected from decarboxylation. Let P = peptide and M = metal. Since we were unable to accurately describe either system [Ca(II) or Mg(II)] with the PM, PM_2, or P_2M (with the Gla side chains of both peptides protected) models, this assumption was reevaluated. Examination of the protection profiles (Figs. 1 and 2) for the lower peptide concentration (0.2 mM) suggests that the PM and the PM_2 species must be protected; whereas, as the peptide concentration was increased, the curves (protection *versus* metal/peptide) take on a sigmoidal shape and, for Ca(II), shift to larger metal to peptide ratios. A previous paper (16) reported a similar sigmoidal shape in the protection profile of Gla in the presence of guanidine (Fig. 4). The sigmoidal shape for the protection of a Gla residue in the presence of guanidine was postulated to be due to the formation of an unprotected species, the 1:1 Gla-guanidine (PG) complex, prior to formation of the protected 1:2 Gla-guanidine (PG_2) complex. By analogy to the guanidine analyses, it can be argued that, in the presence of a low concentration of metal ions, the higher peptide species (P_nM, $n > 1$) is either partially or not at all protected. Therefore, a "protection coefficient" for the P_2M species of the P_2M model was introduced.[2] This expanded P_2M model provided for a better description of all data sets; the PM and PM_2 models were not improved with the addition of the protection coefficient. In the case of Mg(II), the binding constants determined from the data at the three peptide concentrations (0.2, 2.0, and 17.5 mM) were approximately the same. The average equilibrium constants for the three sets provided a good fit of the data. Thus, a model had been found which simulates the Mg(II) ion concentration profiles. Consistency of the Ca(II) equilibrium constants determined for the three peptide concentrations with the P_2M model was somewhat improved, although the fits were still not acceptable. Clearly, Mg(II) and Ca(II) do not bind in an identical manner to the malonyl group of a Gla residue.

In order to better describe the Ca(II) experiments, a P_3M

species was added to the P_2M model; this inclusion (Calculations, Section 6) provided a satisfactory simulation of the calcium data sets when only one of the three malonate subgroups was constrained to be stable to thermal decarboxylation. The P_3M model did not significantly enhance the fit of the Mg(II) data. Thus, binding of both metal ions has been simulated by different models. The Mg(II) data requires the inclusion of a P_2M species in addition to the PM species while the Ca(II) data requires a further additional species, P_3M. In both cases, the higher peptide (P_nM, $n > 1$) species were not completely protected. We conclude that a discernible difference in the binding of Ca(II) and Mg(II) to Gla exists. Both metal ions form a 1:1 complex (PM) that is protected from decarboxylation; it is reasonable that the structure is a chelation bidentate (a form of chelation that involves both carboxylate groups of Gla). The difference found between Mg(II) and Ca(II) appears in the nature of the higher peptide species (P_nM, $n > 1$). In the case of Mg(II), the P_2M species is "unprotected" and both malonate groups are probably in a thermally labile unidentate or bidentate arrangement in which only one carboxylate is involved. For Ca(II), on the other hand, the P_3M species is apparently one-third protected, with one of the malonate subgroups in a stable chelation bidentate type and the remaining malonate subgroups in a labile geometry consistent with either a unidentate or bidentate orientation. There was no evidence in these simulations that Mg(II) forms a P_3M species.

DISCUSSION

Various experimental and theoretical techniques have been utilized in an attempt to study the complexation of Gla residues with metal ions. Among these methods are x-ray crystallography (22–30), fluorescence (31, 32), and various NMR experiments (31, 33–36). These studies have been unable to unambiguously detect a difference between the binding of Ca(II) and of other metal ions, specifically Mg(II).

Thus far, Gla-metal ion complexes have not been successfully examined by x-ray crystallography (22), although the structures of substituted malonic acids have been determined. Curry *et al.* (23) reported the crystal structures of methyl malonate ion with both Mg(II) and Ca(II) ions. These workers reported that the Mg(II)-methyl malonate ion complex is strictly monomeric and octahedral. The Ca(II)-methyl malonate ion complex is polymeric, containing both six and seven coordinate calcium ions with the various methyl malonate ion in all three types of possible ion-binding modes: unidentate, bidentate, and chelation bidentate. The observation that Ca(II) ion-malonate ion derivative complexes can be polymeric, or are not strictly octahedral, has been made by other researchers (24–26). The only other determined crystal structure for a malonate ion complexed with Mg(II) is the bis-(hydromalonato)-magnesium complex (27). This bis complex was found to be monomeric, with both malonate ions in a chelation bidentate orientation and the metal octahedrally coordinated. Thus, although substantial differences in the crystal structures of malonate-metal ion complexes exists, no systematic pattern for Ca(II) and Mg(II) ions binding to the malonate ion emerges.

Differentiation between the binding of these divalent metal ions with substituted malonate ions has also been the subject of several theoretical studies (37–42). These calculations suggest that either metal ion (Ca(II) or Mg(II)) will interact with the malonate ion in a similar manner, specifically, with the metal in a chelation bidentate orientation, although the Mg(II) ion has a somewhat larger calculated binding energy for *in vacuo* complexes.

---

[2] Portions of this paper (including "Theoretical Modeling" and Tables 1 and 2) are presented in miniprint at the end of this paper. Miniprint is easily read with the aid of a standard magnifying glass. Full size photocopies are included in the microfilm edition of the Journal that is available from Waverly Press.

The results of the present analysis of the thermal decarboxylation data suggests that the highly coordinated (presumably tight) sites of the protein will bind Ca(II) with a different coordination behavior than Mg(II) binding. The binding of either metal ion to a single Gla residue (presumably the loose sites) should be similar. Thus Ca(II), by virtue of its larger radius, appears to be able to bind to a greater number of negatively charged ligands than Mg(II). At low metal ion concentrations, Mg(II) may be expected to form uni- or bidentate complexes of the P_2M type, i.e. ($\ldots$ Gla $\ldots$)$_2M$, with protein Gla residues. The 2 Gla residues could come from the same protein chain, from 2 Gla residues on two different protein chains, or both. Ca(II), on the other hand, may form P_3M or even more complex forms.

The dissociation equilibrium constants obtained from the simulation of this data are 1 to 2 orders of magnitude tighter than one would expect based upon equilibrium dialysis data (6, 8, 9, 43, 44) performed at 25 °C. The peptide/metal solutions were frozen in a dry ice/isopropanol bath (−80 °C); therefore, there could be a substantial temperature effect on the thermodynamic equilibrium constants. The relationship of the equilibrium constants determined in this study to constants from an equilibrium dialysis study is not easy to establish; however, our results are highly suggestive of differences in structure between Gla and Ca(II) and Mg(II) complexes.

This study presents new data which, when added to the growing list of other information (6, 9, 23, 24, 43, 44), tends to support the concept that calcium/magnesium ion differences seen in biological systems may be due to the relatively limited coordination sphere of magnesium as compared to calcium.

REFERENCES

1. Suttie, J. W. (1980) *Fed. Proc.* **39**, 2730–2735
2. Furie, B. C., Borowski, M., Keyt, B., and Furie, B. (1982) in *Calcium and Cell Function* (Cheung, W. Y., ed) Vol. II, pp. 217–242, Academic Press, New York
3. Nelsestuen, G. L. (1984) *Metal Ions Biol. Systems* **17**, 353–381
4. Nelsestuen, G. L. (1976) *J. Biol. Chem.* **251**, 5648–5656
5. Suttie, J. W., and Jackson, C. M. (1977) *Physiol. Rev.* **57**, 1–70
6. Prendergast, F. G., and Mann, K. G. (1977) *J. Biol. Chem.* **252**, 840–850
7. Iyengan, G. V., Kollmer, W. E., and Bowen, H. J. (1978) *The Elemental Composition of Human Tissues and Body Fluids*, Verlag Chemie, New York
8. Deerfield, D. W., II, Berkowitz, P., Olson, D. L., Wells, S., Hoke, R. A., Koehler, K. A., Pedersen, L. G., and Hiskey, R. G. (1986) *J. Biol. Chem.* **261**, 4833–4839
9. Deerfield, D. W., II, Olson, D. L., Berkowitz, P., Byrd, P. A., Koehler, K. A. Pedersen, L. G., and Hiskey, R. G. (1978) *J. Biol. Chem.* **262**, 4017–4023
10. Price, P. A., Nelson, C., and Williamson, M. K. (1984) *Anal. Biochem.* **136**, 119–126
11. Tuhy, P. M., Bloom, J. W., and Mann, K. G. (1979) *Biochemistry* **18**, 5842–5848
12. Poser, J. W., and Price, P. A. (1979) *J. Biol. Chem.* **254**, 431–436
13. Stenflo, J., Fernlund, P., Egan, W., and Roepstorff, P. (1974) *Proc. Natl. Acad. Sci. U. S. A.* **71**, 2730–2733
14. Nelsestuen, G. L., Zytkovicz, T. H., and Howard, J. B. (1974) *J. Biol. Chem.* **249**, 6347–6350
15. Magnusson, S., Sottrup-Jensen, L., Petersen, T. E., Morris, H. R., and Dell, A. (1974) *FEBS Lett.* **44**, 189–193
16. Gray, A. L., Hoke, R. A., Deerfield, D. W., II, and Hiskey, R. G. (1985) *J. Org. Chem.* **50**, 2189–2191
17. Bajaj, S. P., Price, P. A., and Russell, W. A. (1982) *J. Biol. Chem.* **257**, 3726–3731
18. Boggs, N. T., III, Bruton, H. D., Craig, D. H., Helpern, J. A., Marsh, H. C., Pegram, M. D., Vandenbergh, D. J., Koehler, K. A., and Hiskey, R. G. (1982) *J. Org. Chem.* **47**, 1812–1816
19. Marki, W., Oppliger, M., and Schwyzer, R. (1977) *Helv. Chim. Acta* **60**, 807–815
20. Marki, W., Oppliger, M., Thanei, P., and Schwyzer, R. (1977) *Helv. Chim. Acta* **60**, 798–806
21. Klapper, G. D. (1982) in *Methods in Protein Sequence Analysis* (Elizinga, M., ed) pp. 509–515, Humana Press, Clifton, NJ
22. Park, C. H., and Tulinsky, A. (1986) *Biochemistry* **25**, 3977–3982
23. Curry, M. E., Eggleston, D. S., and Hodgson, D. J. (1985) *J. Am. Chem. Soc.* **107**, 8234–8238
24. Zell, A., Einspahr, H., and Bugg, C. E. (1985) *Biochemistry* **24**, 533–537
25. Marsh, R. E., and Schomaker, V. (1979) *Inorg. Chem.* **18**, 2331–2336
26. Briggman, B., and Oskarsson, A. (1978) *Acta Crystallogr. Sect. B Struct. Crystallogr. Cryst. Chem.* **34**, 3357–3359
27. Karpides, A., Ault, J., and Reed, A. T. (1977) *Inorg. Chem.* **16**, 3299–3302
28. Satyshur, K., and Rao, S. T. (1977) *Abstracts of the American Crystallography Association, Summer Meeting*, p.74
29. Albertson, J., Oskarsson, A., and Svensson, C. (1978) *Acta Crystallogr. Sect. B Struct. Crystallogr. Cryst. Chem.* **34**, 2737–2743
30. Briggman, B., and Oskarsson, A. (1978) *Acta Crystallogr. Sect. B Struct. Crystallogr. Cryst. Chem.* **34**, 3357–3359
31. Sarasua, M. M., Scott, M. E., Helpern, J. A., Ten Kortenaar, P. B. W., Boggs, N. T., III, Pedersen, L. G., Koehler, K. A., and Hiskey, R. G. (1980) *J. Am. Chem. Soc.* **102**, 3404–3412
32. Marsh, H. C., Sarasua, M. M., Madar, D. A., Hiskey, R. G., and Koehler, K. A. (1981) *J. Biol. Chem.* **256**, 7863–7870
33. Hoke, R. A., Deerfield, D. W., II, Pedersen, L. G., Koehler, K. A., and Hiskey, R. A. (1986) *Int. J. Pept. Prot. Res.* **28**, 569–578
34. Furie, B. C., Blumenstein, M., and Furie, B. (1979) *J. Biol. Chem.* **254**, 12521–12530
35. Sperling, R., Furie, B. C., Blumenstein, M., Keyt, B., and Furie, B. (1978) *J. Biol. Chem.* **253**, 3898–3906
36. Marki, W., Oppliger, M., Thanei, P., and Schwyzer, R. (1977) *Helv. Chim. Acta* **60**, 805–807
37. Gottschalk, K. E., Hiskey, R. G., Pedersen, L. G., and Koehler, K. A. (1981) *J. Mol. Struct.* **76**, 197–201
38. Gottschalk, K. E., Hiskey, R. G., Pedersen, L. G., and Koehler, K. A. (1981) *J. Mol. Struct.* **85**, 337–342
39. Gottschalk, K. E., Hiskey, R. G., Pedersen, L. G., and Koehler, K. A. (1982) *J. Mol. Struct.* **87**, 155–159
40. Gottschalk, K. E., Hiskey, R. G., Pedersen, L. G., and Koehler, K. A. (1982) *J. Mol. Struct.* **108**, 173–178
41. Long, G. A., Hiskey, R. G., Pedersen, L. G., and Koehler, K. A. (1984) *J. Mol. Struct.* **108**, 173–178
42. Maynard, A. T., Hiskey, R. G., Pedersen, L. G., and Koehler, K. A. (1985) *J. Mol. Struct.* **124**, 213–221
43. Olson, D. L., Deerfield, D. W., II, Berkowitz, P., Hiskey, R. G., and Pedersen, L. G. (1987) *Anal. Biochem.* **160**, 468–470
44. Deerfield, D. W., II, Olson, D. L., Berkowitz, P., Koehler, K. A., Pedersen, L. G., and Hiskey, R. G. (1987) *Biochem. Biophys. Res. Commun.* **144**, 520–527

Michael R. Lewis, David W. Deerfield II, Randal A. Hoke, Karl A.
Koehler, Lee G. Pedersen, and Richard G. Hiskey.

THEORETICAL MODELING

Section 1

Theoretical modeling of the experimental data involved:
1. choosing a particular thermodynamic model
2. finding the closest match between the model and
the experiment by optimizing the thermodynamic
binding constant(s).
3. comparing the 'goodness of fit' of this model with
other possible models.

The basic decarboxylation experiment consisted of ten samples
with fixed total peptide concentration ($[P_t]$=0.2, 2.0, or 17.5
mM). Sufficient metal solution (either calcium or magnesium) was
added to each peptide solution to establish a specific ratio of
metal to peptide (molar ratios: 0.0, 0.125, 0.250, 0.333, 0.500,
0.750, 1.0, 2.0, 4.0, and 8.0). The first experimental solution
contained no metal ion and thus provided the amount of
decarboxylation (heating one hour at 110°C) of the other nine samples.
The average 'blank' (experimental point one (ep(1)) gave an
average of 6% decarboxylation; this amount was not a function of
peptide concentration. Saturation was reached at high metal
ion:peptide ratio (an average of 95% protection) and the last
experimental point (ep(10)) was used to represent the average
total amount of "protection".

Since previous observations (16) that the 1:1 complex between Gla
and guanidine decarboxylated at the same rate as Gla itself, we
assume that all "unprotected" species decarboxylated at the same
rate as Gla.

Secondly, we assume that the percentage of Gla remaining after
heating (ep(i)) is the sum of the Gla in "unprotected" and
"protected" species:

Eq 1-1
$$ep(i) = ep(1) * \sum \frac{[\text{"unprotected"}]}{[P_t]} + ep(10) * \sum \frac{[\text{"protected"}]}{[P_t]}$$

This equation provides a basis for the comparing the different
metal forms.

Section 2 - The PM Model

The simplest case for the simulation of the experimental data
allows for a one to one complex between peptide and metal ion:

Eq 2-1
$$P_f + M_f \overset{K_1}{\rightleftharpoons} PM$$
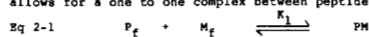
The equilibrium constant can be written as:

Eq 2-2 $K_1 = [P_f]*[M_f]/[PM]$

Where:

Eq 2-3 $[P_f] = [P_t] - [PM]$

Eq 2-4 $[M_f] = [M_t] - [PM]$

substituting equations 2-3 and 2-4 into 2-2 leads to:

Eq 2-5 $K_1 = ([P_t] - [PM])*([M_t] - [PM])/[PM]$

expanding:

Eq 2-6 $K_1*[PM] = [P_t]*[M_t] - [P_t]*[PM] - [M_t]*[PM]$

rearrangement gives:

Eq 2-7 $0 = [PM]^2 - ([M_t] + [P_t] + K_1)*[PM] + [P_t]*[M_t]$

This quadratic has two solutions:

Eq 2-8 $[PM(1)] = ([M_t]+[P_t]+K_1+(([P_t]+[M_t]+K_1)^2-4*[P_t]*[M_t])^{0.5})/2$

Eq 2-9 $[PM(2)] = ([M_t]+[P_t]+K_1-(([P_t]+[M_t]+K_1)^2-4*[P_t]*[M_t])^{0.5})/2$

[PM] must be a bounded real number ($0<[PM]<[P_t]$). In general,
equation 2-9 leads to the correct solution with assumed values
for K_1. Once [PM] is known, equation 2-3 yields the free peptide
concentration [P_f].

In this model, PM is assumed to be "protected". Therefore, the
mole fraction of "protected" species is the mole fraction of the
PM species. P_f is "unprotected" and thus the mole fraction of
"unprotected" species would be the mole fraction of P_f.

The values of $[P_f]$ and [PM] are functions of the assumed K_1. To
check the 'goodness' of the assumed K_1, equation 1-1 is evaluated
with the above assumptions to give a calculated point (cp(i)) for
each metal ion and peptide concentration:

Eq 2-10 $cp(i) = ep(1)*[P_f]_{calc}/[P_t] + ep(10)*[PM]_{calc}/[P_t]$

The difference between the calculated point (cp(i)) and
experimental point (ep(i)) is squared to give the deviation of
the model and the experimental data at that given combination of
$[P_t]$ and $[M_t]$:

Eq 2-11 $SS = (cp(i) - ep(i))^2$

The deviation is then summed over the number of experimental data
points and divided by the degrees of freedom of the model
(n=number of data points, j=variables in the model) to define a
mean square error (MSE):

Eq 2-12 $MSE = \sum_{i=1}^{n} SS / (n - j)$

K_1 was varied until the minimum MSE function was found.

Section 3 - The PM$_2$ Model

The following sequential addition of two metal ions to a single
peptide residue was considered:

Eq 3-1 $P_f + M_f \overset{K_1}{\rightleftharpoons} PM + M_f \overset{K_2}{\rightleftharpoons} PM_2$
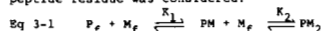
The equilibrium constants can be written as:

Eq 3-2 $K_1 = [P_f]*[M_f]/[PM]$

Eq 3-3 $K_2 = [PM]*[M_f]/[PM_2]$

Rearrangement leads to:

Eq 3-4 $[PM] = [P_f]*[M_f]/K_1$

Eq 3-5 $[PM_2] = [PM]*[M_f]/K_2 = [P_f]*[M_f]*[M_f]/(K_1*K_2)$

In order to calculate the concentrations of PM and PM$_2$, it is
necessary to first determine $[P_f]$ and $[M_f]$. Initially only $[P_t]$
and $[M_t]$ are known. However, assuming values for the equilibrium
constants K_1 and K_2, $[P_f]$ and $[M_f]$ can be determined by
substituting equations 3-4 and 3-5 into the following mass
balanced equations:

Eq 3-6 $[P_t] = [P_f] + [PM] + [PM_2]$

Eq 3-7 $[P_t] = [P_f] + [P_f]*[M_f]/K_1 + [P_f]*[M_f]*[M_f]/(K_1*K_2)$

Eq 3-8 $[M_t] = [M_f] + [PM] + 2*[PM_2]$

Eq 3-9 $[M_t] = [M_f] + [P_f]*[M_f]/K_1 + 2*[P_f]*[M_f]*[M_f]/(K_1*K_2)$

Substitution of the mass balance equations 3-7 and 3-9,
respectively, into the denominator of the following identities:

Eq 3-10 $[P_f] = [P_f]*[P_t]/[P_t]$

Eq 3-11 $[M_f] = [M_f]*[M_t]/[M_t]$

leads to:

Eq 3-12 $[P_f] = [P_f]*[P_t]/([P_f]+[P_f]*[M_f]/K_1+[P_f]*[M_f]*[M_f]/(K_1*K_2))$

Eq 3-13 $[P_f] = [P_t]/(1 + [M_f]/K_1 + [M_f]*[M_f]/(K_1*K_2))$

and

Eq 3-14 $[M_f] = [M_f]*[M_t]/([M_f]+[P_f]*[M_f]/K_1+2*[P_f]*[M_f]*[M_f]/(K_1*K_2))$

Eq 3-15 $[M_f] = [M_t]/(1 + [P_f]/K_1 + 2*[P_f]*[M_f]/(K_1*K_2))$

These equations are solved (Section 6) to give $[P_f]$ and $[M_f]$.
Using equations 3-4 and 3-5, [PM] and [PM$_2$] are calculated. In
this model, it is assumed that PM and PM$_2$ are "protected" and
that P_f is "unprotected". Thus, substitution of the appropriate
mole fractions into equation 1-1 leads to:

Eq 3-16 $cp(i) = ep(1)*[P_f]_{calc}/[P_t]+ep(10)*([PM_2]_{calc}+[PM]_{calc})/[P_t]$

With the assumed K_1 and K_2, a calculated point is found (cp(i))
and compared with the experimental point (ep(i)) to provide a
variance (SS) for each point. These variances are summed over the
data set to determine a specific MSE for each set of K_1 and K_2.
The values for K_1 and K_2 are changed through a sequential grid
search until the minimum in the MSE function is found.

Section 4 - The P$_2$M Model, The Use of the Protection Factor

The third model investigated was one in which a higher order
peptide species was allowed to form, specifically P$_2$M. The
equation is:

Eq 4-1 $P_f + M_f \overset{K_1}{\rightleftharpoons} PM + P_f \overset{K_3}{\rightleftharpoons} PM_2$
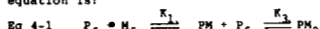
In a manner similar to that outlined in Section 3, the equations
for [PM] and [P$_2$M] are written in terms of $[P_f]$, $[M_f]$, K_1, and
K_3.

Eq 4-2 $[PM] = [P_f]*[M_f]/K_1$

Eq 4-3 $[P_2M] = [P_f]*[P_f]*[M_f]/(K_1*K_3)$

Then, into the mass balanced equations:

Eq 4-4 $[P_t] = [P_f] + [PM] + [PM_2]$

Eq 4-5 $[M_t] = [M_f] + [PM] + 2*[PM_2]$

were substituted equations 4-2 and 4-3. the resulting mass
balanced equations were then substituted into the identities 3-10
and 3-11 to yield:

Eq 4-6 $[P_f] = [P_t]/(1 + [M_f]/K_1 + 2*[P_f]*[M_f]/(K_1*K_3))$

Eq 4-7 $[M_f] = [M_t]/(1 + [P_f]/K_1 + [P_f]*[P_f]/(K_1*K_3))$

Equations 4-6 and 4-7 are solved by the iterative method (See
Section 6) and [PM] and [P$_2$M] are calculated with appropriate
equations (equations 4-2 and 4-3). It is necessary to define
whether each species is "protected" from thermal decarboxylation.
From previous results it was obvious that P_f is "unprotected" and
that PM is "protected" from decarboxylation. It is, however, not
obvious whether P$_2$M would be "protected". Since there are two
peptide residues per metal ion, the total complex could be
totally "unprotected", half "protected", or totally "protected".
In the simulation of the data, each of these possibilities was
examined and a new variable was introduced - Fl. Fl has three
possible values: 0-unprotected, 0.5-half protected,
1.0-protected. Therefore, the equation for the protected species
is modified to:

Eq 4-8 $[\text{"Protected"}] = (2*Fl*[P_2M] + [PM])/[P_t]$

If Fl represents the amount "protected", then (1-Fl) represents
the amount "unprotected". Modification of the unprotected species
equation yields:

Eq 4-9 $[\text{"Unprotected"}] = (2*(1-Fl)*[P_2M] + [P_f])/[P_t]$

Substituting equations 4-8 and 4-9 into equation 1-1 leads to:

Eq 4-10 $cp(i)=ep(1)*([P_f]+2*(1-Fl)*[P_2M])/[P_t]+ep(n)*(2*Fl*[P_2M]+[PM])/[P_t]$

Thus, for any combination of K_1 and K_3, it is necessary to
evaluate 4-10 for the three possible values of Fl. There are,
therefore, three different cp's (cp1(i), cp2(i), and cp3(i), that
lead to three different variances.

Eq 4-11 $SS(1) = (ep(i)-cp(1)(i))^2$

Eq 4-12 $SS(2) = (ep(i)-cp(2)(i))^2$

Eq 4-13 $SS(3) = (ep(i)-cp(3)(i))^2$

Each of these variances is summed over the data set and then the
sum is divided by the degrees of freedom in the model (n-j, where
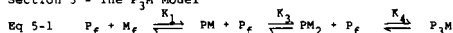n=number of data points, j=variables in the model=3 (K_1, K_3, and
Fl)) to define the MSE:

Eq 4-14 $MSE(1) = (\sum_{i=1}^{n} SS(1))/(n-j)$

Eq 4-15 $MSE(2) = (\sum_{i=1}^{n} SS(2))/(n-j)$

Eq 4-16 $MSE(3) = (\sum_{i=1}^{n} SS(3))/(n-j)$

K_1 and K_3 were systematically varied through a grid search until the minimum MSE value was found.

Section 5 - The P_3M Model

Eq 5-1 $P_f + M_f \underset{K_1}{\overset{}{\rightleftharpoons}} PM + P_f \underset{K_3}{\overset{}{\rightleftharpoons}} PM_2 + P_f \underset{K_4}{\overset{}{\rightleftharpoons}} P_3M$

Into the mass balance equation:

Eq 5-2 $[P_t] = [P_f] + [PM] + 2*[P_2M] + 3*[P_3M]$

one substituted the appropriate equations (equations 4-2 and 4-3) and:

Eq 5-3 $[P_3M] = [P_f]*[P_f]*[P_f]*[M_f]/(K_1*K_3*K_4)$

to give:

Eq 5-4 $[P_t] = [P_f] + [P_f]*[M_f]/K_1 + 2*[P_f]*[P_f]*[M_f]/(K_1*K_3) + 3*[P_f]*[P_f]*[P_f]*[M_f]/(K_1*K_3*K_4)$

Substituting equation 5-4 into the denominator of equation 3-10 and then simplifying yields:

Eq 5-5 $[P_f] = \dfrac{[P_t]}{1+[M_f]/K_1+2*[P_f]*[M_f]/(K_1*K_3)+3*[P_f]*[P_f]*[M_f]/(K_1*K_3*K_4)}$

In a similar manner, equation 5-6 is found:

Eq 5-6 $[M_f] = \dfrac{[M_t]}{(1+[P_f]/K_1+[P_f]*[P_f]/(K_1*K_3)+[P_f]*[P_f]*[P_f]/(K_1*K_3*K_4))}$

It was found that $[P_f]$ and $[M_f]$ were easily calculated with the iterative method (see Section 6) using equations 6-5 and 6-6. After $[P_f]$ and $[M_f]$ are found, one then calculates $[PM]$, $[P_2M]$, and $[P_3M]$ with equations 4-2, 4-3, and 5-3.

It is assumed that PM is "protected" and P_f is "unprotected"; it is necessary to evaluate the amount of "protection" for P_2M and P_3M. As before (Section 5), P_2M could either be "unprotected" (F1=0), half "protected" (F1=0.5), or totally "protected" (F1=1). Therefore, the contribution for P_2M to the "protected" species is $2*F1*[P_2M]$ and to the "unprotected" species is $2*(1-F1)*[P_2M]$.

For the P_3M species, there are three peptide residues in the metal complex. The overall complex can either be "unprotected" (F2=0), have only one residue protected (F2=1/3), two residues protected (F2=2/3), or have all residues protected (F2=1). Therefore, the contribution to the "protected" species due to P_3M is $3*F2*[P_3M]$ and the "unprotected" species is $3*(1-F2)*[P_3M]$.

Substituting the appropriate terms into equation 1-1 leads to:

Eq 5-6 $cp(i) = ep(1)*([P_f]+2*F1*[P_2M]+3*F2*[P_3M])/[P_t] +$
$\qquad\qquad ep(10)*([PM]+2*(1-F1)*[P_2M]+3*(1-F2)*[P_3M])/[P_t]$

Thus, for any combination of K_1, K_3, and K_4, it is necessary to also evaluate the 12 different combinations of F1 and F2 (F1= 0, 1/2, 1; F2= 0, 1/3, 2/3, 1), which results in twelve different calculated points, thus twelve different variances. These variances are summed over the data set. The MSE error is calculated and the minimum is found by systematically varying K_1, K_3, and K_4 in a sequential grid search.

Section 6 - Different Methods for Calculating $[P_f]$ and $[M_f]$

There are at least three different ways to solve equations 3-13 and 3-15.

Eq 3-13 $[P_f] = [P_t]/(1 + [M_f]/K_1 + [M_f]*[M_f]/(K_1*K_2))$

Eq 3-15 $[M_f] = [M_t]/(1 + [P_f]/K_1 + 2*[P_f]*[M_f]/(K_1*K_2))$

Section 6.A - Analytical Method

The first method involves the analytical solution of a polynomial in $[M_f]$ derived as follows:

Eq 6-1 $[M_f] = [M_t]/(1 + [P_f]*(1/K_1 + 2*[M_f]/(K_1*K_2)))$

and then substitution of 3-13 into 6-1 leads to:

Eq 6-2 $[M_f]=[M_t]/$
$\quad (1+[1/K_1+2*[M_f]/(K_1*K_2))*([P_t]/(1+[M_f]*(1/K_1+[M_f]/(K_1*K_2)))$

Expanding and rearranging leads to:

Eq 6-3 $[M_f]^3+(K_2+2*[P_t]-[M_t])*[M_f]^2+K_2*(K_1+[P_t]-[M_t])*[M_f]-K_1*K_2*[M_t]=0$

Equation 6-3 is in the cubic form of $y^3 + py^2 + qy + r$, where:

Eq 6-4 $p = K_2 + 2*[P_t] - [M_t]$

Eq 6-5 $q = K_2*(K_1 + [P_t] - [M_t])$

Eq 6-6 $r = K_1*K_2*[M_t]$

this is this converted to the form of $x^3 + ax + b = 0$, where:

Eq 6-7 $y = x-p/3$

Eq 6-8 $a = (3*q - p^2)/3$

Eq 6-9 $b = (2*p^3 - 9*p*q + 27*r)/27$

In general, there are three solutions for this equation:

Eq 6-10 $[M_f(1)] = 2*((-a/3)^{1/2})*\cos(\alpha/3) - p/3$

Eq 6-11 $[M_f(2)] = 2*((-a/3)^{1/2})*\cos(\alpha/3 + 2*\pi/3) - p/3$

Eq 6-12 $[M_f(3)] = 2*((-a/3)^{1/2})*\cos(\alpha/3 + 4*\pi/3) - p/3$

where:

Eq 6-13 $\alpha = \arccos((-b/2)*((-a^3/27)^{1/2}))$

There are several difficulties with this method: The first problem is the obvious necessity of deciding which root (Eq 6-10, 6-11, or 5-12) is within the reasonable limits of $[M_f]$ (i.e., $0<[M_f]<[M_t]$). Even within a series of calculations, the reasonable root will change. Another problem concerns the evaluation of the arc cosine function. Most micro-computers do not evaluate $\arccos(x)$; but instead, one must convert into an arc-tan(y) (atn) function:

Eq 6-14 $\arccos(x) = 1.570796 - atn(x/sqr(1-x*x))$

Although for all values of x, $\arccos(x)$ is defined, arctan is not (when x=1, the denominator is equal to 0). Consequently, error trapping in the computercode is necessary. The code necessary for a program using the analytical method is, at best, cumbersome. This leads to both programming difficulties and increased computational time. Solving the analytical polynomials for more complex thermodynamic equilibrium equations is impractical.

Section 6.B Newton's Method

The second solution utilizes Newton's iterative method of succesive approximations:

Eq 6-15 $[M_f](i+1) = [M_f](i) - F(i)/F'(i)$

where F(i) is a function of $[M_f]$. When a solution is found, F(i)=0. In this case, F(i) is equal to equation 6-3, that is:

Eq 6-16 $F(i) = [M_f]^3+(K_2+2*[P_t]-[M_t])*[M_f]^2+K_2*(K_1+[P_t]-[M_t])*[M_f]-K_1*K_2*[M_t]$

F'(i) is the first derivative of F(i)

Eq 6-17 $F'(i) = 3*[M_f]^2+2*(K_2+2*[P_t]-[M_t])*[M_f]+K_2*(K_1+[P_t]-[M_t])$

An inital $[M_f]$ is guessed, equations 6-16 and 6-17 are evaluated and then these values are used in equation 6-16 to calculate a new $[M_f]$. With the new $[M_f]$ from 6-15, equations 6-16 and 6-17 are again evaluated and a new $[M_f]$ is calculated. This process is continued until a convergence criteria is met (e.g., $([M_f](i+1)-[M_f](i))/[M_f]<0.001$). The advantage of this method is that the programming is simple and the calculations are relatively fast. The disadvantages are: 1.) This method does not always converge, but will occasionally lead to oscillations, 2.) the convergent solution may not be within reasonable limits of $[M_f]$ (i.e., $0<[M_f]<[M_t]$), or 3.) the convergent solution may depend upon the starting point if there are multiple roots close to the reasonable limits (See Section 6.A).

Section 6.C The Iterative method

We have found the most reliable procedure to be an iterative method that simultaneously solves equations 3-13 and 3-15. Initial estimates of $[P_f]$ and $[M_f]$ are used to start the iterative cycle. New $[P_f]$ and $[M_f]$ values are obtained from 3-13 and 3-15, and used in the next cycle. Again, a convergence criterion is used. The essential code (in BASIC) is:

Eq 6-18   FOR I=1 TO 100
Eq 6-19   PF = PT/(1 + MF/K1 + MF*MF/K1/K2)
Eq 6-20   MF = MT/(1 + PF/K1 + 2*PF*MF/K1/K2)
Eq 6-21   IF ABS(1-PMF/MF)<0.001 THEN I=100
Eq 6-22   PMF=MF
Eq 6-23   NEXT I

The advantages are: 1.) regardless of the complexity of the model or starting point in the calculation, the values of $[P_f]$ and $[M_f]$ converge rapidly, 2.) the solution is always a real and reasonable number within the appropriate boundaries, 3.) the computer code is simple and the equations for larger models are easily developed. Therefore, this iterative method was used in all calculations, except for the PM model. (For a similar procedure, see ref 43.)

TABLE 1
Results of Curve Fitting Analysis for Thermal Decarboxylation of
γ-Carboxyglutamic Acid in the presence of Ca(II)
(All equilibrium constants are dissociation constants (mM))
MSE is defined in the text. The average data set's equilibrium
constants are the average of the three data sets equilibrium
constants. The MSE Ave. is the deviation of each data set when
the averaged equilibrium constants are used.

Model	[Gla]	K_1	K_2	K_3	K_4	F1	F2	MSE	MSE Ave.
PM	0.2	0.0045						19.7	2687
	2.0	0.59						7.3	271
	17.5	7.0						60.0	177
	Ave.	2.53							3135
PM$_2$	0.2	0.004	95.0					23.3	3361
	2.0	0.47	7.95					7.9	398
	17.5	7.95	1.70					16.0	124
	Ave.	2.81	34.88						3883
P$_2$M	0.2	0.004		95.0				23.4	3247
	2.0	0.47		7.9				5.7	336
	17.5	7.00		900.0				72.0	187
	Ave.	2.49		334.0					3770
P$_2$M	0.2	0.0025	1.67	6.5		1.0		39.2	2250
	2.0	0.144	0.50	16.5		1.0		2.68	39
	17.5	0.975	8.0	2.9		0.0		4.47	217
	Ave.	0.374	3.39	8.6		0.0			2506
P$_3$M	0.2	0.0053		0.013	0.28	0.5	0.33	0.1	2
	2.0	0.0085		0.038	0.15	0.0	0.33	0.4	3
	17.5	0.0066		0.050	0.18	0.5	0.33	1.3	9
	Ave.	0.0068		0.034	0.20	0.5	0.33		14

TABLE 2
Results of Curve Fitting Analysis for Thermal Decarboxylation of
γ-Carboxyglutamic Acid in the presence of Mg(II)
(All equilibrium constants are dissociation constants (mM))
MSE is defined in the text. The average data set's equilibrium
constants are the average of the three data sets equilibrium
constants. The MSE Ave. is the deviation of each data set when
the averaged equilibrium constants are used.

Model	[Gla]	K_1	K_2	K_3	K_4	F1	F2	MSE	MSE Ave.
PM	0.2	0.005						1.5	421
	2.0	0.34						26.2	30
	17.5	0.10						62.1	81
	Ave.	0.15							532
PM$_2$	0.2	0.005	5.5					1.8	127
	2.0	0.13	0.27					25.6	41
	17.5	0.0005	0.40					67.5	90
	Ave.	0.045	2.06						258
P$_2$M	0.2	0.007		2.7				1.3	2462
	2.0	0.75		70.				29.9	280
	17.5	3.10		1900.				72.0	194
	Ave.	1.286		657.					2936
P$_2$M	0.2	0.006	12	2.7		0.0		2.1	10
	2.0	0.022	7.5	2.5		0.0		3.0	31
	17.5	0.002	12.0	6.5		0.0		11.2	42
	Ave.	0.010	10.5	3.9		0.0			83